New and Promising Techniques Using Fiber Bragg Grating Sensors for Horse Gait Analysis

José Rodolfo Galvão; André Biffe Di Renzo; Pedro Esber Schaphauser; Alessandra Kalinowski; John Canning; Carlos R. Zamarreño, *Member, IEEE*; Jean Carlos Cardozo da Silva and Cicero Martelli.

***Abstract*—This article presents two in vivo instrumentation techniques to study the different types of gaits of horses performing athletics using fiber Bragg gratings (FBG). These techniques can be used as an auxiliary tool in the early diagnosis of injuries related to the horse's locomotor system, mainly in the distal portion of the digit, one of the most common causes of retirement when they are athletes. Therefore, the first technique presented consists of the fixation of FBGs without encapsulation, directly on the dorsal wall of the hoof in each of the limbs. In the second technique presented, the FBG sensor is encapsulated in a prototype developed using a composite material reinforced with carbon fiber in a horseshoe shape. The second technique is associated with digital image processing (DIP) for better visualization of the deformation and compression forces that act upon the limbs. The first method showed sensitivity to detection of the digit compression against the ground, being able to identify walking patterns. The second technique, with the encapsulated sensor elements, also allows the capture of characteristic signals of gait, such as step walk, trot, and gallop under training conditions. These two techniques of instrumentation using FBGs sensors, the second associated with DIP, are promising for the clinical and biomechanical study and medical evaluation of horses even during dynamic training and competition.**

***Index Terms* — equine gaits, athlete horse, equine hoof, biosensor, Bragg gratings, in vivo monitoring, optical-fiber sensors.**

I. Introduction

LIMB pathologies, especially in their distal portions, are considered to be the most common cause of decreased performance and medical care in horses performing athletics [1]–[5], with lameness (limp) being the first clinical sign presented by the animal [3], [5]–[7]. Pathologies such as laminitis and navicular syndrome are frequent causes of retirement and even euthanasia of animals [4], [8], [9], generating a millionaire loss. The income generated in the Agribusiness Complex of the Horse in Brazil, in April 2015, totaled R$ 16.15 billion. The Agribusiness of the Horse complex directly employs 607,329 people. Considering the fact that each direct occupation provides four other indirect occupations, it is estimated that 2,429,316 indirect jobs are generated [10]. According to the American Horse Council, in 2005, the horse industry contributed approximately $39 billion in direct economic impact to the U.S. economy and supports 1.4 million jobs on a full- time basis. When indirect and induced spending are included, the industry's economic impact reaches $102 billion.

The effects of different hardening methods on the hoof wall have been studied [2], [11], [12], together with the biomechanics of healthy hooves [13]–[15]. Together, they are considered the key point for success sought by the different forms of treatment, as well as being of extreme importance for the understanding and prevention of these two diseases so present in the equine clinic.

The most commonly used method for lameness diagnosis is the clinical presentation and visual evaluation of the animal when performing certain procedures. Therefore, the diagnosis depends on the practice and sensitivity of the veterinarian evaluator [5], [7], [16], [17]. The disagreement between evaluators increases significantly in less severe lameness, especially when they come from the pelvic limbs [7].

In vivo measurement of forces induced by equine hooves using strain gauges (SGs) have been reported [18]–[20]. To monitor small deformations, SGs represent a consistent and highly tested technology; they offer good sensitivity, accurate measurements, and at a competitive price. However, despite the results presented in these studies [18]–[20], SGs have some disadvantages for in vivo use. They cannot be left at the measurement site [21], their miniaturization features for minimally invasive procedures present some drawbacks such as long-term fragility and instability [22], [23]. In addition, the detection by SGs is restricted to a small area of sensitivity, making it necessary to use more sensors to scan larger regions. As a result, a large number of electrical wires may represent a considerable foreign body [21], [24], [25]. These disadvantages combined with poor biocompatibility of metallic components

Commented [JC2]: Brazil or whole world?

Commented [JC3]: Wow quite big!

Commented [JC1]: Is this an actual name of an organization or a widely used acronym term?

Manuscript was received on March 05, 2018. This work was supported in part by the Brazilian Agencies CNPq, CAPES, FINEP, Fundação Araucária, and SETI and the Spanish Economy and Competitiveness Ministry-Feder TEC2013-43679-R and José Castillejo 2015 Research Grants.

J. R. Galvão, A. B. Di Renzo, P. E. Schaphauser, A. Kalinowski, C. Martelli, and J. C. C. Silva are affiliated with the Federal University of Technology–Parana, Curitiba 80230-901, Brazil (phone: +55 4133104741; e-mail: jgalvao@utfpr.alunos.edu.br; cmartelli@utfpr.edu.br; jeanccs@utfpr.edu.br).

J. Canning is with the University of Technology, Sydney, Australia.

C. R. Zamarreño are affiliated with the Electrical and Electronic Engineering Department, Public University of Navarra, Pamplona, NA 31006, SPAIN (phone: +34 948168445; fax: +34 948169720; e-mail: carlos.ruiz@unavarra.es).

and high sensitivity to electromagnetic interference may compromise some in vivo applications and the use of SGs in clinical practice.

Fiber optic sensors have great potential for applications in biomechanics because of the advantages of silica fibers, such as small dimensions, in the order of micrometers in diameter and millimeters in length, biocompatibility, nontoxicity, and chemical inertia [26], [27]. In addition, fiber Bragg grating (FBG) sensors are intrinsically safe for in vivo application; i.e. their use does not produce any interference in the homeostasis of animals.

The horseshoe or hoof of the animal instrumented with FBGs generate data that allow the evaluation of different types of walking, in real time, and can help in the monitoring of different lameness configurations that the animal can present. Both techniques of instrumentation using FBG sensors are new and promising in this field of equine biomechanics.

Just as videos are used to analyze movements of athletes to verify and improve their performance [28], this same idea can be used in competition horses to verify possible stress points in the animal members. Therefore, in parallel to the collection of FBG signals, videos of the horse moving were recorded with fuzzy logic recognizing colors in the captured images. This identification allows a visual analysis of the mechanical deformation exercised by the animal during it's gait, identifying every member of the horse and inserting colors based on the FBGs signals [29]. This technique can be used in rapid identification of possible health problems.

This article presents the methodology of optical hoof instrumentation, the manufacture of a horseshoe with FBGs sensors integrated in carbon fiber composite material, a software to recognize walking patterns, and the results of tests performed on two horses of the Crioula breed. The tests were followed by a veterinarian and approved by the Ethics Committee on Animal Use of the Federal University of Technology - Paraná (protocol CEUA 2016-027).

II. METHODOLOGY

This section describes the methodology adopted for the optical instrumentation of the horse. The steps carried out were: instrumentation of the horse's hooves, confection and installation of the horseshoe in a carbon composite, development of a software to evaluate the deformation of the horseshoes instrumented through a color map, and finally the procedures of field trials.

A. Instrumentation of hooves

For the instrumentation of the horse's hooves, four FBGs were used in different optical cables. A horse of the Crioula breed participated of the tests, which realized trot walking on a concrete floor without a mounted rider.

The FBGs were fabricated with different wavelengths using an Excimer laser (Coherent, Xantos-XF-ArF, operating at wavelength of 193 nm), using four phase masks with respective wavelengths: λ = 1527.00, 1532.00, 1553.00, and 1568.00 nm. All sensors has a reflectivity of $R \sim 60\%$. After recording, each FBG sensor was fixed directly to the horse's hoof wall, upright, in the middle third of the wall [30], [31], according to the schematic representation of Fig. 1.

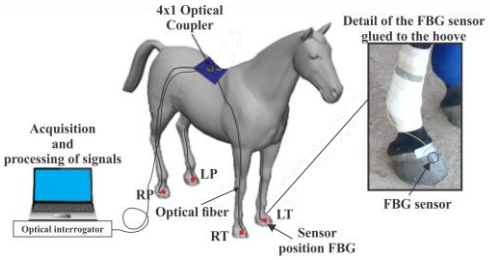

Figure 1. Schematic drawing of the hooves optical instrumentation.

For a better fixation of the sensors, the hoof was sanded and sanitized with alcohol. The FBGs sensors were fixed using cyanoacrylate-based glue. To avoid tension on the FBG sensor at the time of fixation, the limb was suspended in the air; this procedure was repeated for the other thoracic and pelvic limbs. The optical cable of the FBG sensor was guided on each thoracic and pelvic limb with the aid of adhesive tapes, later they were connected to a 4x1 optical coupler, which was fixed on the saddle of the horse. A 20-meter optical extension was used to connect the optical coupler to the interrogation system. In this experiment, the optical interrogator SM130 from Micron Optics® was used, with a 1 kHz acquisition rate (wavelength stability 2 pm and wavelength repeatability 1 pm), connected to a notebook for data recording. For analysis of the results, the signal from each sensor was named as follows: RT - right thoracic limb; LT - left thoracic limb; RP - right pelvic limb; LP - left pelvic limb.

B. Carbon fiber horse shoe

Horse shoes were manufactured using 10 layers of carbon fiber fabric, which were bidirectional (200 g/m2). Epoxy resin, thermosetting type, was used for lamination on a flat surface. FBG sensors were added in the middle of the 10 layers of carbon fiber, that is, between the fifth and the sixth layer. In this experiment, we used FBG sensors recorded in an Excimer laser, as described in item II-A, with the following wavelengths: 1556.00, 1560.00, 1564.00, and 1568.00 nm. Each FBG was installed in one shoe. For better mechanical strength, the shoe was inserted into a vacuum bag, and held for 1 hour at 80ºC and for 8 hours at 140ºC. The final finishing was carried out according to the dimensions of the horse's hooves that would be tested.

The horsehoes were installed on a horse of the Crioula breed. The tests were performed on a sand lane, and the horse ran in clockwise circles. To obtain the data, a 4x1 optical coupler connected to the IMON512e optical interrogator from Ibsen Photonics® (970 Hz acquisition frequency and 0.5 pm resolution) was used. The interrogator was connected to a laptop to read the data and transmit it via wireless. A second laptop, fixed on a bench, was used to receive the data and manage the records. The schematic drawing is shown in Fig. 2.

Commented [JC4]: Presumably there is also an impact if any salt from swat gets in since it changes conductivity as well as create dampness

Commented [JC5]: Good stuff

Commented [JC6]: Crioulo? Is there a feminine form of this?

Commented [JC7]: Do you need two decimal places here?

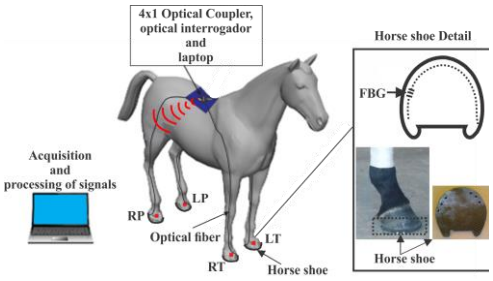

Figure 2. Schematic drawing of the horsehoe instrumented in carbon composite.

For better viewing the acquired signals by the FBG sensors, a video of the horse movements was made. This video was synchronized with the acquisition of the signals by the optical interrogator. To record the video, an unmanned aerial vehicle (UAV) DJI Inspire 1 RAW with rotary wing and a coupled camera DJI X5R was used. This camera has 16 Mpixels, 4096 x 2160 pixels of resolution, acquisition of 24 frames per second, and is stabilized in the three axis, providing pictures without trembling. With the need to acquire the images to make a later analysis of the gait, this video was processed to insert the information obtained from the FBG sensors. It is important to have a platform that allows a clear image acquisition and also to be able to easily move it with the animal to get every detail. Because of this necessity, the UAV with a coupled camera was the better option to capture the equine movements.

To insert information from the FBG sensors in the video, it was necessary to identify the points of interest. After the identification of these points, they were replaced by colors that represent the collected signals from the FBG sensors. The DIP technique was used to identify every marked member of the horse. Among various techniques to identify points of interest, in this study used color segmentation. Because there are four horse members, we have four points of interest. Thus, each member was bandaged with a distinct color band. For better understanding, Fig. 3 shows the horse making one of the movements with the bands and the FBG sensors. The technique used to identify each point of interest in the picture was performed with fuzzy logic.

Figure 3. Picture of the horse with the limbs bandaged with distinct colors.

To identify specific colors in images, one of the first steps is to choose what space color to use to process the image. Normally, digital cameras acquire images in the red, green, blue (RGB) space color [32]. However, this color space is complex to identify specific colors. Therefore, a better choice is the Hue-Saturation-Value (HSV). In this space color, all colors are defined in the H channel. With this, it is only necessary to select the color by the H channel and the saturation and brightness by the S and V channels [29].

With a less complex space color, fuzzy logic can be used to precisely identify specific colors [29]. To identify some color, it is first necessary to define the membership function that represents the color to be identified. This function will verify if the analyzed color has or does not have the characteristics of the color to be found. A membership function to identify colors in the HSV space color is described by Eq. 1:

$$\text{IF} \quad (H_B \leq H \leq H_A) \wedge (S_B \leq S \leq S_A) \wedge (V_B \leq V \leq V_A) \quad \text{SO} \tag{1}$$

where H represents the Hue channel, S represents the Saturation channel, V the value (brightness) channel of the space color HSV, and the "Λ" represents a logical "AND". The letters "A" and "B" above each channel represents the high and low limits for each color to be identified [29]. The technique of identifying colors by fuzzy logic was applied in a routine that reads each pixel of a picture. In the case where the specific colors of the horse limbs satisfy Eq. 1, these pixels were marked to receive information of the FBG sensors. However, because the pictures were acquired in an environment that did not have a luminosity control; therefore, identification errors could occur. Another point that can cause error is dirt in the bands, thus modifying the band color. To suppress these errors, morphological closing was used, cleaning unwanted points [32].

After identifying the limbs, the FBG sensors' signals were converted into colors that represents the horseshoes deformations during the movements. In this step, the data was normalized to standardize the color scale of each limb. After the normalization, the color scale was defined from the high and low deformation identified in a set of movements. The high deformation was colored with red and the low deformation with blue. Thus, the color scale starts in the blue color and ends in the red color, using other colors to represents the intermediary values that occur in the equine movementation. Through this process, it is possible to analyze beyond the captured movements in the video, the occurring deformations during the walk. This makes it possible to develop a diagnosis of lameness with agility during the activities of the horse and even during a competition.

III. Results and Discussion

The following paragraphs describe the experiments performed using the two proposed methods. Item A presents the results of hooves instrumentation experiments. Item B presents the results of the experiment with the instrumented shoes, for

step walking, trotting, and galloping. The experiments are intended not to evaluate the animal, but the optical instrumentation system.

A. Results of hooves instrumentation experiments

The experiment result with the instrumented hoof is shown in Fig. 4. This experiment occurred with the horse in trotting gait, straight, on a level concrete floor. Fig. 4 shows the deformation of the hoof detected by the four sensors, and it is possible to observe the repetition of a pattern in the signal for both the thoracic and the pelvic limbs.

At point A, we highlight the initial support phase of the RP, which is the moment of the first impact on the ground. At that time, the response of the FBG sensor glued to the hoof wall in the region of the middle third of the dorsal plane of the hoof, moves to values of negative deformation, indicating that the hull suffered compression, because of phalangeal rotation movements [33]. To illustrate the positioning of the phalange inside the hoof, Fig. 5 shows a sagittal cut of the equine digit. Still at point A, the other limbs are suspended in the air. At point B, the maximum deformation for the RP, which is the ground support phase, has the greatest mass discharge on the limb. The LP is still hanging in the air. The LT is supported on the ground (impact phase). At point C, the rolling phase of the RP and LT stands out, there is a marked oscillation of the signal for the RP, and a larger magnitude oscillation for the LT. These oscillations can again be justified by phalangeal movements during the bearing phase of the support phase. At point D, the members RP and RT are suspended in the air and at point E, the cycle repeats, now with the LP and RT in ground support phase and the RP and LT suspended in the air. The results show that the sensors are sensitive to detections of digit compression against the ground, exerted by the skeleton on the phalanges and the shell of the hoof during the support phase, reproducing signals similar to those found by Thomason et al. (1992) [18]. Although with advantages over the system presented, because FBG sensors use less cables, providing greater comfort to the animal, the monitoring can therefore be done at several points of all the limbs simultaneously.

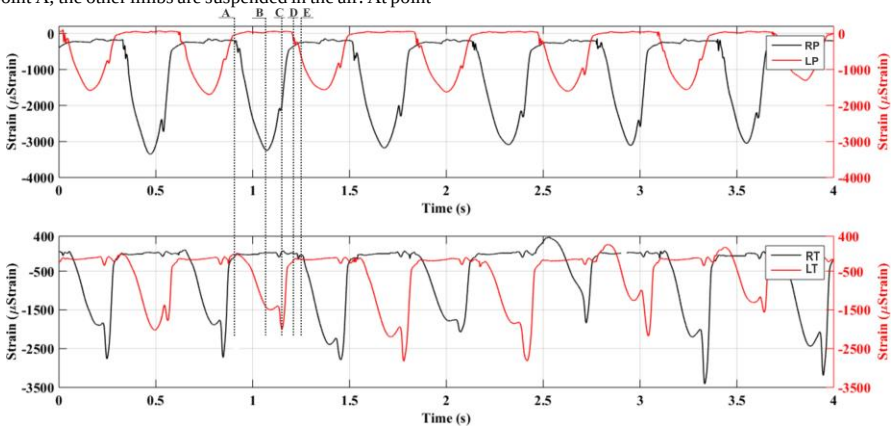

Figure 4. Deformations generated on the hooves of their respective limbs during the monitoring of gait-like gait in relation to time.

B. Horseshoe instrumented in carbon composite

The experiment using the instrumented horseshoes focused on the comparison of the results obtained from the FBGs sensors in different types of gait: step walk, trot, and gallop.

Figure 6 shows the strain variation (μStrain) as a function of time, for walking step. For better understanding, in each graph are highlighted four points. In particular, at point A, the beginning of the support phase of the RP, which is the moment of the first impact of the limb on the ground and the end of the bearing limb of the LP, is highlighted at that moment; the RT is suspended in the air, even as the LT is supported on the ground (support stage). At point B, the moment when the RT touches the ground is highlighted, the impact phase being with the soil, and the LT is still in contact with the ground for a few seconds in the rolling phase. Point C highlights a slight oscillation in the signal of the RP; this may be justified by the limb being in the swing state with the RT, there being a slight relief of pressure on the RP. At point D, it terminates the step of supporting the RP and initiates the step of supporting the LP, whereas the LT is suspended in the air and the RT remains in the intervening step of support. At point E, the moment when the LT initiates the support phase stands out; it is noted that the RT is still in the final support phase. This behavior is consistent when we analyze step gait, reported in the literature [33]–[35]. Note the repetition of the FBG sensor signals in the thoracic and pelvic limbs.

The differences in amplitude of the signals are because of several factors that may have occurred during the test, such as: (i) the horse walked on a sand floor, causing the hoof to sink into the ground during the passes, consequently changing the distribution of force around the hoof; (ii) the rider executed the pitch in a circle clockwise, with a difference in the force distribution of each limb; (iii) there may be a small space gap between the horseshoe and the hoof.

Figure 7 shows strain variation (μStrain) as a function of time (s), for trot gait. In the highlighted point A, the beginning phase of the support of the RP and LT is reached, highlighting the

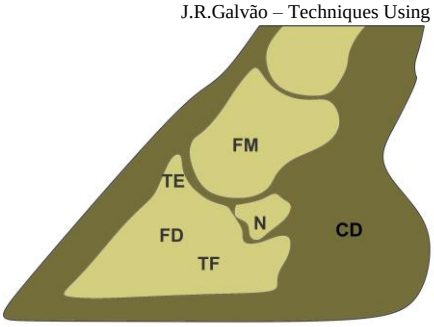

Figure 5. Schematic drawing of the distal portion of a thoracic digit in a sagittal section. Where: (FM) distal portion of the medial phalange; (FD) distal phalange; (N) navicular bone; (CD) digital cushion; and the distal portions of extensor (TE) and flexor (TF) tendons.

initial phase of preimpulse. At point B, the maximum force point of LT and RP is obtained, even as RT and LP are suspended in air. At point C, it reverses the sequence of the bearing sides of the limbs, the LT and RP being suspended in the air, and the RT and LP initiating the preimpact.

At point D, the maximum deformation peak for LP and RT is highlighted. Finally, point E represents the beginning of a new cycle of the limb support phase. This sequence of support of the limbs is coherent with reports in the literature [33]–[35]. Comparing these data with step gait, we notice a decrease in the interval of the support phases, which is normal, considering that the velocity increases, and we notice a difference in the sequence of the stages of support of the limbs, also coherent with data in literature [33]–[35].

Figure 8 shows the strain variation (μStrain) as a function of time (s), for gallop gait. The galloping gait is considered to be of greater velocity when compared to step and trot gait. Note on the recorded signals a decrease in the time interval when the limb touches the ground. At point A, the RP initiates the presupport phase along with the LT, even as the LP is in the final swing phase, and the RT is suspended in the air. At point B, the final step of support of the RP and LT is reached, and the RP and LT are now suspended, initiating the support phase only of the LP. At point C, it is interesting to note that in a few seconds, all members are suspended in the air. At this point, the strain variation is close to zero. At point D, the RP and LT have first contact with the ground, even as the others are still suspended in the air. Finally, at point E, the cycle of the support phases begins again, repeating the whole sequence. Again, there is a difference in the pattern of the gait phase, which is consistent for this type of gait.

In parallel to the acquisition of the signs, the video of the equine movements was recorded and the technique to identify the bands was executed. Thus, after the identification of the limbs, the sensor information was converted to a color scale and the information was inserted in the places of the bands in the picture. The obtained result can be visualized in the Fig.9.

In this picture, it is possible to see the color scale used to represent the exercised deformations, positioned in the left top corner. To visualize the deformations measured by the sensors, beyond the color representation, the chart was added at the top right corner showing the values measured. In the bottom of the picture, specific in the portions that have the animal limbs, a zoomed image is applied allowing a better visualization. From the processed image, it is possible to visualize more quickly the deformations made by the animal during the gait, allowing the identification of painful points.

Using the DIP to unify the captured pictures of the animal movements with the sensors signals, it is possible to identify movements that could make injuries. In addition, it is be possible to verify actual injuries that need to be treated or to identify muscle stress that can cause some injury.

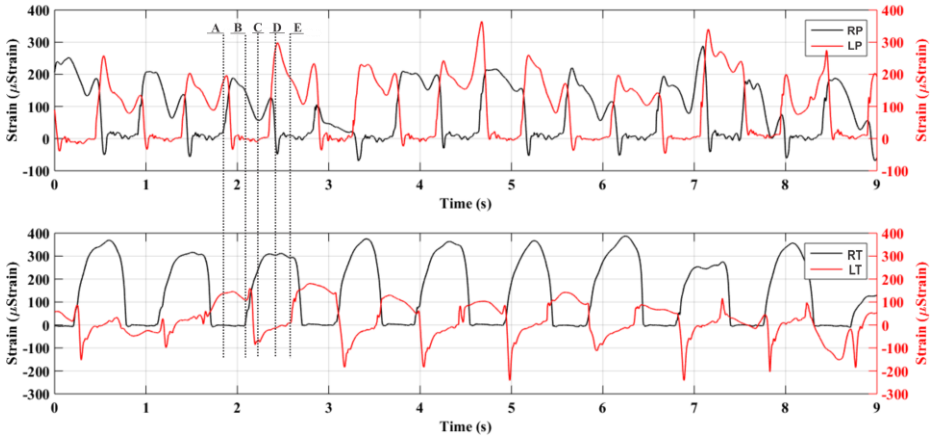

Figure 6. Variation of the strain of the four horseshoes instrumented with FBGs sensors for step gait.

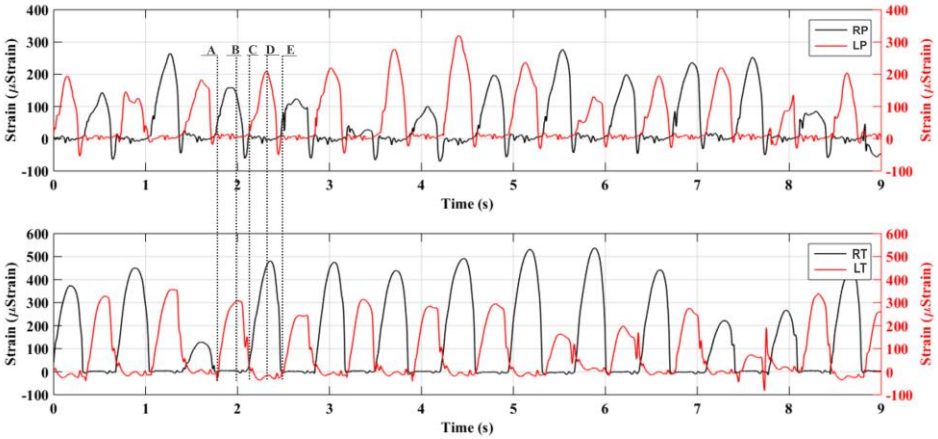

Figure 7. Variation of the strain of the four horseshoes instrumented with FBGs sensors for trot gait.

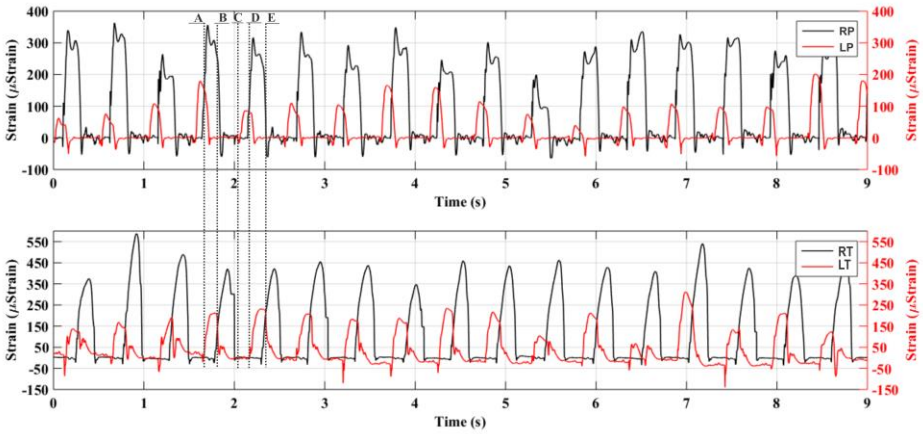

Figure 8. Variation of the strain of the four horseshoes instrumented with FBGs sensors for gallop gait.

IV. Conclusions

This article presents optical hooves instrumentation, the manufacture of a horseshoe with FBGs sensors integrated in carbon fiber composite material, and a software for pattern recognition. Fiber optic sensors have great potential for applications in the field of equine biomechanical analysis, are minimally invasive, biocompatible, chemically inert, and are more comfortable for animal use because it uses fewer cables than electrical sensors.

The results obtained with the sensors glued directly to the hooves showed sensitivity to the detection of the digit compression against the ground, being able to identify the intensity of the compression and deformation as well as frequency of the step, that is, walking patterns. The results obtained with the sensor encapsulated in composite material show that with this technique it was also possible to capture characteristic signals of each gait, presenting the advantage of reuse of the sensors, as the horseshoe where the sensor is encapsulated can be removed and placed again when desired.

The technique of optical instrumentation with the sensor encapsulated in composite material associated to the digital image processing is new and promising for the area of biomechanics.

By recognizing and characterizing the gait patterns for a healthy animal, it is possible to monitor animals during their daily activities and thus be able to recognize abnormal patterns and avoid possible lameness diseases. This monitoring can be carried out by a veterinarian, or by the owner of the animal, during the day, or even during a sporting event, being able to avoid more serious injuries and consequent early retirement of

the animal in his life of competition.

ACKNOWLEDGMENT

This work was supported in part by the Brazilian Agencies CNPq, CAPES, FINEP, Fundação Araucária, SETI, the Spanish Economy and Competitiveness Ministry-Feder TEC2016-78047-R, and José Castillejo 2015 Research Grants.

REFERENCES

[1] J. Thomason, W. Bignell, D. Batiste, and W. Sears, "Effects of hoof shape, body mass and velocity on surface strain in the wall of the unshod forehoof of standardbreds trotting on a treadmill," *Equine and Comparative Exercise Physiology*, vol. 1, no. 2, pp. 87–97, 2004.

[2] N. Hansen, H. F. Buchner, J. Haller, and G. Windischbauer, "Evaluation using hoof wall strain gauges of a therapeutic shoe and a hoof cast with a heel wedge as potential supportive therapy for horses with laminitis," *Veterinary Surgery*, vol. 34, no. 6, pp. 630–636, 2005.

[3] G. M. Baxter, *Adams and Stashak's Lameness in Horses*, 6th ed., G. M. Baxter, Ed. Colorado: Wiley-Blackwell, 2011.

[4] J. Lefroy, "Navicular syndrome: Using new technology to unlock the secrets of this complex lameness," *Canadian HORSE HEALTH Annual*, pp. 46–50, 2013.

[5] C. Goulet, J. Olive, Y. Rossier, and G. Beauchamp, "Radiographic and anatomic characteristics of dorsal hoof wall layers in nonlaminitic horses," *Veterinary Radiology and Ultrasound*, vol. 56, no. 6, pp. 589– 594, 2015.

[6] H. M. Clayton, D. Sha, J. Stick, and N. Elvin, "3d kinematics of the equine metacarpophal-angeal joint at walk and trot," *Veterinary and Comparative Orthopaedics and Traumatology*, vol. 20, pp. 86–91, 2007.

[7] M. Hammarberg, A. Egenvall, T. Pfau, and M. Rhodin, "Rater agreement of visual lameness assessment in horses during lungeing," *Equine veterinary journal*, vol. 48, no. 1, pp. 78–82, 2016.

[8] T. S. Stashak *et al.*, *Adams' lameness in horses.* Verlag M. & H. Schaper, 2008.

[9] I. Grundmann, W. T. Drost, L. J. Zekas, J. K. Belknap, R. Garabed, S. Weisbrode, A. Parks, M. Knopp, and J. Maierl, "Quantitative assessment of the equine hoof using digital radiography and magnetic resonance imaging," *Equine veterinary journal*, vol. 47, no. 5, pp. 542–547, 2015.

[10] R. d. S. LIMA and A. CINTRA, "Revisão do estudo do complexo do agronegócio do cavalo," *Ministério da Agricultura, Pecuária e Abastecimento, Brasília*, vol. 56, 2015.

[11] H. S. Cheramie and S. E. O'Grady, "Hoof repair and glue-on shoe adhesive technology," *Veterinary Clinics of North America: Equine Practice*, vol. 19, no. 2, pp. 519–530, 2003.

[12] M. Hüppler, F. Häfner, S. Geiger, D. Mäder, and J. Hagen, "Modifying the surface of horseshoes: effects of eggbar, heartbar, open toe, and wide toe shoes on the phalangeal alignment, pressure distribution, and the footing pattern," *Journal of Equine Veterinary Science*, vol. 37, pp. 86–97, 2016.

[13] M. Oosterlinck, L. Hardeman, B. Van Der Meij, S. Veraa, J. Van Der Kolk, I. Wijnberg, F. Pille, and W. Back, "Pressure plate analysis of toe–heel and medio-lateral hoof balance at the walk and trot in sound sport horses," *The Veterinary Journal*, vol. 198, pp. e9–e13, 2013.

[14] M. Estrada, "Artículo de revisión fundamentos de podología equina: Recorte balanceado y herraje fisiológico," *Revista Ciencias Veterinarias*, vol. 29, no. 2, pp. 41–55, 2014.

[15] K. Les´niak, J. Williams, K. Kuznik, and P. Douglas, "Does a 4-6 week shoeing interval promote optimal foot balance in the working equine?" *Animals*, vol. 7, no. 4, p. 29, 2017.

[16] K. Keegan, E. Dent, D. Wilson, J. Janicek, J. Kramer, A.acarrubba, D. Walsh, M. Cassells, T. Esther, P. Schiltz *et al.*, "Repeatability of subjective evaluation of lameness in horses," *Equine veterinary journal*, vol. 42, no. 2, pp. 92–97, 2010.
A. M. McCracken, J. Kramer, K. Keegan, M. Lopes, D. Wilson, S. Reed, LaCarrubba, and M. Rasch, "Comparison of an inertial sensor system of lameness quantification with subjective lameness evaluation," *Equine veterinary journal*, vol. 44, no. 6, pp. 652–656, 2012.

[17] J. Thomason, A. Biewener, and J. Bertram, "Surface strain on the equine hoof wall in vivo: implications for the material design and functional morphology of the wall," *Journal of Experimental Biology*, vol. 166, no. 1, pp. 145–168, 1992.

[18] Y. H. Chang, J. Sherrill, and J. E. Bertram, "Hoof wall function in horses and donkeys: Experimental alteration of surface strain," in *Bioengineer- ing Conference, 1993, Proceedings of the 1993 IEEE Nineteenth Annual Northeast*. IEEE, 1993, pp. 64–65.

[19] J. Thomason, "Variation in surface strain on the equine hoof wall at the midstep with shoeing, gait, substrate, direction of travel, and hoof shape," *Equine Veterinary Journal*, vol. 26, pp. 86–95, 1998.

[20] T. Fresvig, P. Ludvigsen, H. Steen, and O. Reikeras, "Fibre optic Bragg grating sensors: An alternative method to strain gauges for measuring deformation in bone," *Medical Engineering & Physics*, vol. 30, no. 1, pp. 104–108, 2008.

[21] P. Roriz, L. Carvalho, O. Frazão, J. L. Santos, and J. A. Simões, "From conventional sensors to fibre optic sensors for strain and force measurements in biomechanics applications: A review," *Journal of Biomechanics*, vol. 47, pp. 1251–1261, January 2014.

[22] A. G. Mignani and F. Baldini, "Biomedical sensors using optical fibres," *Reports on Progress in Physics*, vol. 59, pp. 1–28, 1996.

[23] B. Faramarzi, "Quantifying the equine hoof's response to loading during exercise," Ph.D. dissertation, University of Guelph, Guelph, Ontario, Canada, 2007.

[24] J. W. Arkwright, N. G. Blenman, I. Underhill, S. A. Maunder, M. M. Szczesniak, P. G. Dinning, and I. J. Cook, "In-vivo demonstration of a high resolution optical fiber manometry catheter for diagnosis of gastrointestinal motility disorders." *Optics Express*, vol. 17, no. 6, pp. 4500–4508, Mar 2009.

[25] V. Mishra, N. Singh, U. Tiwari, and P. Kapur, "Fiber grating sensors in medicine: Current and emerging applications," *Sensors and Actuators A: Physical*, vol. 167, no. 2, pp. 279–290, 2011.

[26] L. Carvalho, N. J. Alberto, P. S. Gomes, R. N. Nogueira, J. L. Pinto, and
M. H. Fernandes, "In the trail of a new bio-sensor for measuring strain in bone: osteoblastic biocompatibility," *Biosensors & Bioelectronics*, vol. 26, no. 10, pp. 4046–4052, 2011.

[27] R. P. Dubois, D. V. Thiel, and D. A. James, "Using image processing for biomechanics measures in swimming," *Procedia Engineering*, vol. 34, pp. 807–812, 2012.

[28] L. Caponetti and G. Castellano, *Fuzzy Logic for Image Processing: A Gentle Introduction Using Java*. Springer, 2017.

[29] A. Stachurska, R. Kolstrung, M. Pieta, P. Silmanowicz, and
A. Klimorowska, "Differentiation between fore and hind hoof dimensions in the horse (equus caballus)," *Archiv für Tierzucht*, vol. 51, no. 6, pp. 531–540, 2008.

[30] K. D. Budras, W. O. Sack, and S. Röck, *Anatomy of the Horse: with Aaron Horowitz and Rolf Berg*. Schlütersche, 2012.

[31] J. Beyerer, F. Puente León, and C. Frese, *Machine Vision*. Berlin, Heidelberg: Springer Berlin Heidelberg, 2016. [Online]. Available: http://link.springer.com/10.1007/978-3-662-47794-6

[32] C. da Rocha Torres, "As andaduras do cavalo," Curitiba - PR, 1998. [Online]. Available: http://www.centauro.net.br/artigos/AS%20ANDADURAS%20DO%20CAVALO.pdf

[33] A. M. de Andrade, "Biometria e locomoção de equinos da raça brasileiro de hipismo," Master's thesis, Universidade Federal Rural do Rio de Janeiro, 2014.

[34] J. F. d. A. Lôbo *et al.*, "Análise conformacional dos equinos utilizados na equoterapia do centro de reabilitação e readaptação doutor henrique santillo, goiânia, goiás," 2016.